JOURNAL OF BACTERIOLOGY, Apr. 2006, p. 2383–2391 Vol. 188, No. 7
0021-9193/06/$08.00+0 doi:10.1128/JB.188.7.2383–2391.2006

Nucleotide-Dependent Dimerization of the C-Terminal Domain of the ABC Transporter CvaB in Colicin V Secretion

Xiangxue Guo,[1] Robert W. Harrison,[1,2] and Phang C. Tai[1]*

Department of Biology[1] and Department of Computer Sciences,[2] Georgia State University, Atlanta, Georgia 30303

Received 22 December 2005/Accepted 19 January 2006

The cytoplasmic membrane proteins CvaB and CvaA and the outer membrane protein TolC constitute the bacteriocin colicin V secretion system in *Escherichia coli*. CvaB functions as an ATP-binding cassette transporter, and its C-terminal domain (CTD) contains typical motifs for the nucleotide-binding and Walker A and B sites and the ABC signature motif. To study the role of the CvaB CTD in the secretion of colicin V, a truncated construct of this domain was made and overexpressed. Different forms of the CvaB CTD were found during purification and identified as monomer, dimer, and oligomer forms by gel filtration and protein cross-linking. Nucleotide binding was shown to be critical for CvaB CTD dimerization. Oligomers could be converted to dimers by nucleotide triphosphate-Mg, and nucleotide release from dimers resulted in transient formation of monomers, followed by oligomerization and aggregation. Site-directed mutagenesis showed that the ABC signature motif was involved in the nucleotide-dependent dimerization. The spatial proximity of the Walker A site and the signature motif was shown by disulfide cross-linking a mixture of the A530C and L630C mutant proteins, while the A530C or L630C mutant protein did not dimerize on its own. Taken together, these results indicate that the CvaB CTD formed a nucleotide-dependent head-to-tail dimer.

CvaB is an ATP-binding cassette (ABC) transporter from *Escherichia coli* that is responsible for the export of protein toxin colicin V (10). ABC transporters are ubiquitous in eukaryotic and prokaryotic cells. More than 80 ABC proteins, about 5% of the genome, were identified in *E. coli* K-12 (15). Some human genetic disorders, like cystic fibrosis and Wegener's granulomatosis, are due to mutations in ABC transporters (2), and there are at least 48 ABC transporter genes in humans (6). Therefore, it is important to understand the mechanism and structure of ABC transporters.

ABC transporters consist of at least two domains, a nucleotide-binding domain (NBD) and a transmembrane domain (TMD). The functional transporter consists of at least a dimer of the NBD (18). The NBDs show significant sequence similarity and structural homology, while the TMDs do not (38). The lack of homology in the TMDs reflects the wide range of compounds for which export and import are controlled by ABC transporters. ABC transporters control the export or import of compounds such as cytotoxins, antibiotics, antifungal agents, herbicides, and anticancer drugs (14). The structural homology of the NBDs reflects the underlying common mechanism where hydrolysis of a nucleotide triphosphate provides the energy for substrate transport across the cell membrane (17).

The crystal structures of ABC NBDs in both eukaryotes and prokaryotes have been determined, including HlyB (36, 47), MalK (5) from *E. coli*, MJ0796 from *Methanococcus jannaschii* (45), HisP from *Salmonella enterica* serovar Typhimurium (22), GlcV from *Sulfolobus solfataricus* (42), LmrA from *Lactococcus lactis* (PDB accession code 1MV5; provided by Y.-R. Yuan et al.), TAP1 from *Homo sapiens* (9), and the cystic fibrosis transmembrane conductance regulator from *Mus musculus* (28). Two whole ABC transporters have been crystallized, i.e., the lipid transporter MsbA (3, 4, 33) and the vitamin B_{12} importer BtuCD in *E. coli* (30).

The NBD structures show significant structural similarity. The consensus structure is an alpha/beta fold (25). One of the most striking features of the NBD structure is that the highly conserved Walker A and B sites, as well as the ABC signature motif and Q loop, form parts of the nucleotide-binding site and are critical for the function of the ABC transporter (26, 29, 37). However, these motifs are not adjacent to each other in the monomer structure. Clearly, the monomer cannot be the active ABC molecule, and therefore, the factors that control dimer formation are potentially important in understanding the function of the ABC transporters. The canonically accepted model for the role of the NBD in ABC transporters is a chemical pump. The Rad50 crystal structure (19) and the MJ0796 NBD structure (45) with nucleotide triphosphates or triphosphate analogs showed that the NBD dimers formed the nucleotide-binding site. This leads to the hypothesis that nucleotide binding is essential for the formation of dimers, which supplies the "power stroke" for ABC transporter pumps. It is necessary to construct a soluble NBD in order to test this hypothesis, and such a system can be constructed from the *E. coli* CvaB protein (23, 49).

CvaB is part of the dedicated type 1 exporter for export of the bacterial toxin colicin V. This exporter consists of the cytoplasmic membrane proteins CvaA and CvaB and outer membrane protein TolC (10). The CvaB NBD is located at the C terminus and has nearly all of the conserved sites from ABC transporters, including the Walker A (G^{526}ASGAGKT) and Walker B (I^{650}LFMDE) sites (16), the Q loop (Q^{574}), the H switch (H^{684}), and the ABC signature motif (L^{630}SGGQ). The most homologous NBD with a high-resolution crystal structure is the α-hemolysin exporter HlyB (36), where the sequence

* Corresponding author. Mailing address: Department of Biology, Georgia State University, 24 Peachtree Center Avenue, 402 Kell Hall, Atlanta, GA 30303. Phone: (404) 651-3109. Fax: (404) 651-2509. E-mail: biopct@langate.gsu.edu.

TABLE 1. Bacterial strains and plasmids used in this study

Strain or plasmid	Genotype or description	Reference or source
E. coli strains		
DH5α	K-12 *supE44* Δ*lacU169* (ϕ80 *lacZ*ΔM15) *hsdR17 recA1 endA1 gyrA96 thi-1 relA1*	11
BL21	B F^- *ompT* $hsdS_B$	40
Plasmids		
pHK11	pBR322 with *cvaABC* and *cvi*	41
pTrcHisB	Expression vector in *E. coli* with *trc* promoter and N-terminal His6 tag	Invitrogen
pXG11	CvaB-CTD (amino acids 459–698) gene on pTrcHisB between BamHI and EcoRI sites	This study
pXG530	CvaB-CTD mutation Ala^{530} to Cys (A530C) at Walker A site	This study
pXG630	CvaB-CTD mutation Leu^{630} to Cys (L630C) in ABC signature motif	This study
pXG654	CvaB-CTD mutation Asp^{654} to His (D654H) at Walker B site	49

similarity is about 61% (17). While this work was in progress, the nucleotide binding and monomer-dimer equilibrium of the HlyB NBD were reported (1). In solution, the monomer and dimer were in equilibrium and dimer fraction could be increased by adding ATP (48). The ATPase activity of the HlyB NBD showed clear positive cooperativeness (1). Unlike HylB, CvaB showed a preference for GTP at low temperatures (49). Cross-linking studies suggested that there might be a CvaB dimer in vivo (23).

In this paper, we describe the effects of nucleotide binding on the CvaB C-terminal domain (CTD). The CvaB CTD construct was overexpressed and purified, and the role of nucleotide binding in the monomer-dimer equilibrium was investigated. The relative orientation of the two monomers in the dimer was studied by designing a disulfide bridge between the Walker A site and the ABC signature motif (31). Based on these experiments, a functional model is proposed for the role of nucleotide-dependent CvaB dimerization in colicin V secretion.

MATERIALS AND METHODS

Bacterial strains, plasmids, media, chemicals, and reagents. All of the *E. coli* strains used in this study are described in Table 1. Bacterial culture medium TA (10 g of tryptone, 5 g of NaCl, 40 mM potassium phosphate buffer [pH 7.0], 7.6 mM ammonium sulfate, 1.6 mM sodium citrate per liter) was used for both liquid and solid (with 1.5% agar) plates. The antibiotic ampicillin was used at a final concentration of 100 μg/ml. Restriction enzymes, T4 DNA ligase, and EDTA-free protease inhibitor (Roche Applied Sciences) were used essentially as recommended by the manufacturers. All other chemicals were reagent grade and were purchased from Sigma unless otherwise noted.

Plasmid construction, protein expression, and purification. The *cvaB* gene was from plasmid pHK11 (41), and the wild-type and mutant forms of the *cvaB* CTD were constructed on expression vector pTrcHisB (Invitrogen) between the BamHI and EcoRI sites. The vector carried a DNA fragment encoding 31 extra amino acids, which contained six histidines as an Ni^{2+}-binding domain, as used previously in our laboratory (49). Recombinant DNA manipulations were performed essentially as previously described (35). For high-level expression, the constructed plasmids were freshly transformed into the host, *E. coli* BL21. The overnight cell culture of the transformant was diluted 40 times into fresh TA medium, cultivated at 37°C until the optical density at 600 nm reached between 0.4 and 0.6, and induced by 0.5 mM isopropyl-β-D-thiogalactopyranoside (IPTG) at various temperatures for 4 h. The induced cells were harvested, resuspended in affinity binding buffer (25 mM phosphate-buffered saline buffer [pH 8.0], 100 mM KCl, 200 mM NaCl, 7 mM β-mercaptoethanol, 20% glycerol), and passed through a French press (GE Healthcare) twice at 12,000 lb/in^2. The CvaB CTD was purified from cell supernatant through Ni-nitrilotriacetic acid (NTA) affinity chromatography (QIAGEN), Q-Sepharose FF ion-exchange chromatography, and Superose 6 gel filtration chromatography (Pharmacia). The molecular sizes of the different forms were identified by gel filtration chromatography on Superdex 75 HR 10/30 (Pharmacia) in buffer containing 20 mM HEPES (pH 7.6), 100 mM NaCl, 10% glycerol, and 1 mM dithiothreitol (DTT). The purified proteins were stored in aliquots at −80°C in 100 mM 3-(cyclohexylamino)-1-propanesulfonic acid (CAPS) buffer (pH 10.4)–20% glycerol–10 mM DTT.

Site-directed mutagenesis. Plasmid DNA isolation, digestion, transformation, and other routine DNA manipulations were done as previously described (35). Mutagenesis was performed by overlap extension PCR (21) with pHK11 as the *cvaB* gene template. *cvaB* CTD forward and reversed primers 5′-CGCGGATCCAATGAGTCTGCACAATGA and 5′-CGCGAATTCTTAAATAGAAATAACTCT (incorporated BamHI and EcoRI restriction sites are underlined), respectively, and mutant 5′ primers A530C (5′-GCTTCCGGTTGCGGAAAAACC) and L630C (5′-GAAGGTTGTTCTGGCGGT) were used. PCR conditions were 95°C for 5 min; 28 cycles of denaturation at 95°C for 45 s, annealing at 56°C for 30 s, and extension at 72°C for 1 min; and then an extra extension for 10 min by PCR enzyme *Pfu* (Pharmacia). The parent plasmid and newly (PCR) synthesized DNA fragments were digested separately by BamHI and EcoRI. They were then ligated and transformed into *E. coli* DH5α. DNA sequencing was performed with an ABI 377 Sequencer (Applied Biosystems) to verify the mutations and the rest of the DNA sequence.

Gel electrophoresis and Western blotting. sodium dodecyl sulfate (SDS)-polyacrylamide gel electrophoresis (PAGE) (10%) was performed by the method of Laemmli (27). Proteins were transferred to polyvinylidene difluoride membranes (Applied Biosystems) and treated for Western blotting (35) with a polyclonal antibody for the CvaB CTD (49). Alkaline phosphatase-conjugated goat anti-rabbit immunoglobulin G (Bio-Rad) was used as the secondary antibody.

1-Ethyl-3-(3-dimethylaminopropyl)carbodiimide hydrochloride (EDC) cross-linking. The protocol used for EDC cross-linking was that recommended by the manufacturer (Pierce). Protein samples at 1.0 μg/μl in reaction buffer [100 mM 2-(*N*-morpholino)ethanesulfonic acid (MES; pH 5.5), 5 mM GTP, 5 mM $MgCl_2$, 5% glycerol, 1 mM DTT] were preincubated on ice for 5 min and at 25°C for 1 min before a final concentration of 4 mM EDC was added. Cross-linked samples were taken at various times, and the reaction was stopped by adding 1/10 volume of 2 M Tris-HCl (pH 6.8). The cross-linked protein samples were run on SDS-PAGE and identified by Western blotting with CvaB antibodies (49).

Dimerization and dissociation assays. To test the effect of nucleotide binding on protein dimerization, the purified oligomer fraction of the CvaB CTD (30 μg/ml) was incubated at 4°C with 10 mM GTP-Mg^{2+} for various times in 20 mM HEPES buffer (pH 7.6) with 5% glycerol and 1 mM DTT. To determine the effect of nucleotide-magnesium release on the dissociation of protein, the nucleotide-bound CvaB CTD dimer (30 μg/ml) was incubated at 20°C with 15 mM EDTA for various times in 10 mM CAPS buffer (pH 10.4) with 5% glycerol and 1 mM DTT. Finally, each sample was subjected to analytical gel filtration chromatography (Superdex 75 PC 3.2; Amersham) at a flow rate of 0.2 ml/min at 4°C.

Disulfide cross-linking. The disulfide cross-linking procedures used were previously described (34). After freshly removing the DTT from protein stock through gel filtration chromatography, 48-μl protein samples at 2.5 μg/μl in 20 mM HEPES buffer (pH 7.6) were mixed with 12 μl of 15 mM $CuSO_4$, 45 mM 1,l0-phenanthroline, 50 mM sodium phosphate (pH 7.3), and 10% glycerol. The samples were incubated at 37°C for 10 min or as indicated. The reactions were stopped by addition of SDS sample buffer (125 mM Tris-HCl [pH 6.8], 20% glycerol, 4% SDS) containing 50 mM EDTA without reducing agent. The reaction mixtures were subjected to SDS-PAGE (10%) and Western blotting (49).

RESULTS

Both dimers and oligomers of the CvaB CTD were observed. Previous studies in our laboratory (49) utilized constructs expressing the CTD of CvaB (residues 439 to 698) with either a His_6 tag or the gene for glutathione *S*-transferase fused to the N terminus. However, this construct formed inclusion bodies easily. In this study, we constructed several shorter versions of the CTD with 190, 200, 210, 220, 230, and 240 residues. The expression vector pTrcHisB has been used widely for its convenience of purification through Ni^{2+} binding. Although there were 31 extra amino residues, including the six histidines located at the N terminus of the expressed protein, our previous work indicated that they did not affect the protein's nucleotide binding or hydrolysis activity (49). IPTG induction was per-

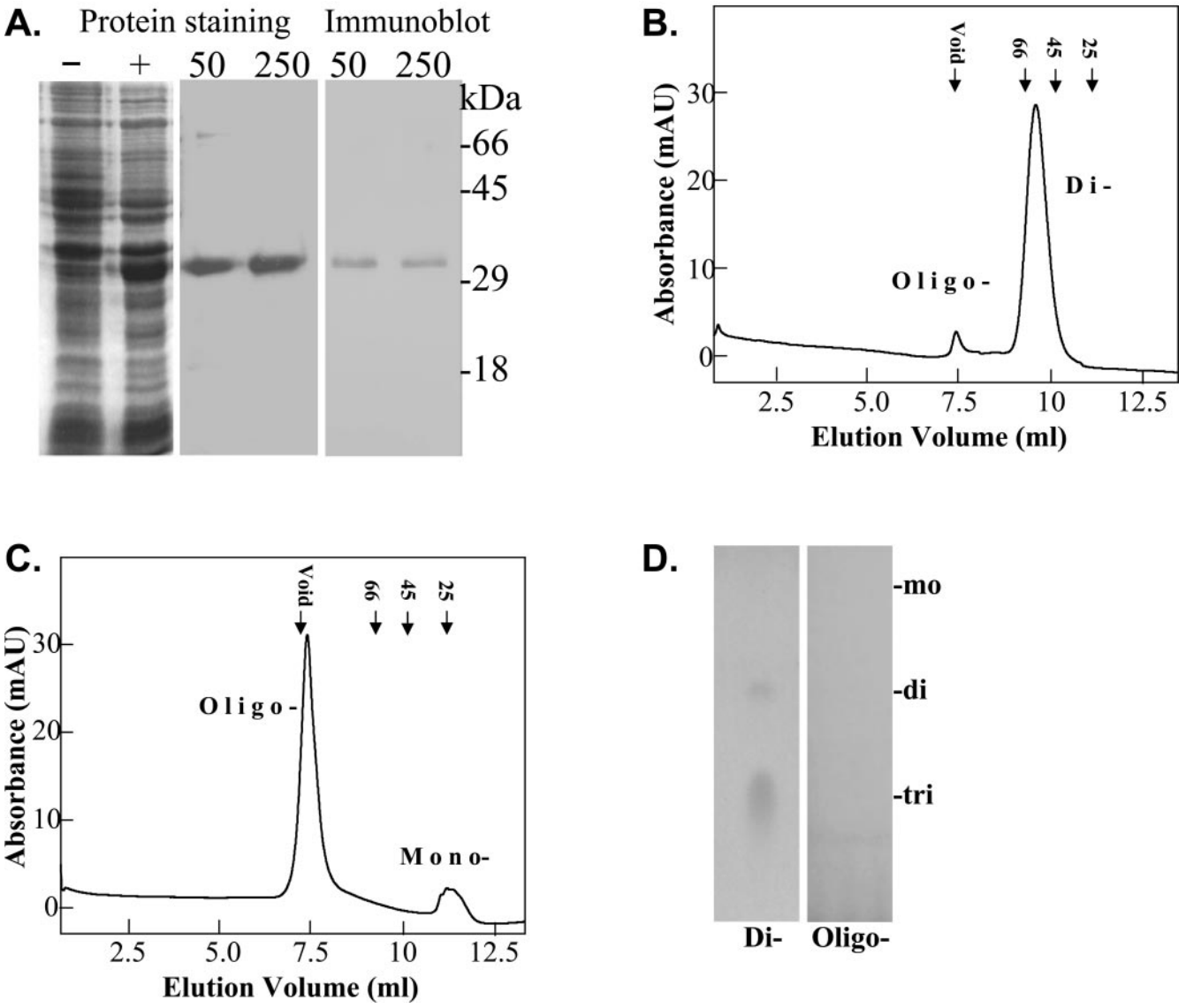

FIG. 1. Purification of different forms of the CvaB CTD. The purity of CTDs and immunoblots is shown in panel A (with and without IPTG induction; fractions eluted with 50 and 250 mM imidazole). The CTD dimer and oligomer were eluted by 50 mM (B) and 250 mM (C) imidazole (oligo, oligomer; di, dimer; mo, monomer). Molecular mass markers: void, blue dextran 2000; 66 kDa, albumin; 45 kDa, ovalbumin; 25 kDa, chymotrypsinogen. (D) Nucleotides bound with the CTD dimer shown by fluorescent illumination of TLC plates (nucleotide standards: mo, GMP; di, GDP; tri, GTP). Protein fractions were incubated in boiling water for 2 min, and then the denatured protein was removed by centrifugation. About 0.5 μl of each concentrated supernatant was spotted onto TLC plates (silica gel IB-F254/365 nm, 2.5 by 7.5 cm; J. T. Baker Corp.) at room temperature and developed with isopropanol-H_2O-NH_4OH (10:8:2 [vol/vol]) for 1 h. The sample nucleotides on the air-dried plate in comparison to known nucleotide standards were observed in the UV spectrum at a wavelength of 365 nm.

formed at 27.5°C, which was found to be the optimal temperature for expression and prevention of the formation of excess inclusion bodies. When expressed in *E. coli* BL21 with 0.5 mM IPTG induction, the 240-residue CTD (residues 459 to 698) had better expression and remained more soluble than others in the cytoplasm. This protein was purified through Ni-NTA affinity, ion-exchange, and gel filtration chromatography to more than 99% purity. Two forms of the CvaB CTD were isolated; one eluted at 50 mM and the other eluted at 250 mM imidazole on Ni-NTA chromatography. The apparent molecular mass of the CvaB CTD monomers of both forms was 32 kDa on SDS-PAGE, and both forms were confirmed by immunoblotting (Fig. 1A). The 50 mM imidazole-eluted fraction was about 62 kDa and was identified as a dimer of the CvaB CTD in 20 mM HEPES buffer (pH 7.6) by analytical gel filtration chromatography (Fig. 1B). The A_{280}/A_{260} UV absorbance ratio of the purified dimer fraction was 1.35, indicating the existence of a nucleotide bound to the purified CvaB CTD dimer. Based on calculation, the molecular ratio of protein to nucleotide was close to 1:1, suggesting that two nucleotides were bound to each CvaB CTD dimer. On the other hand, the fraction of the CvaB CTD eluted by 250 mM imidazole was identified as oligomers that appeared at the void volume on the gel filtration column (Fig. 1C). The A_{280}/A_{260} ratio of the

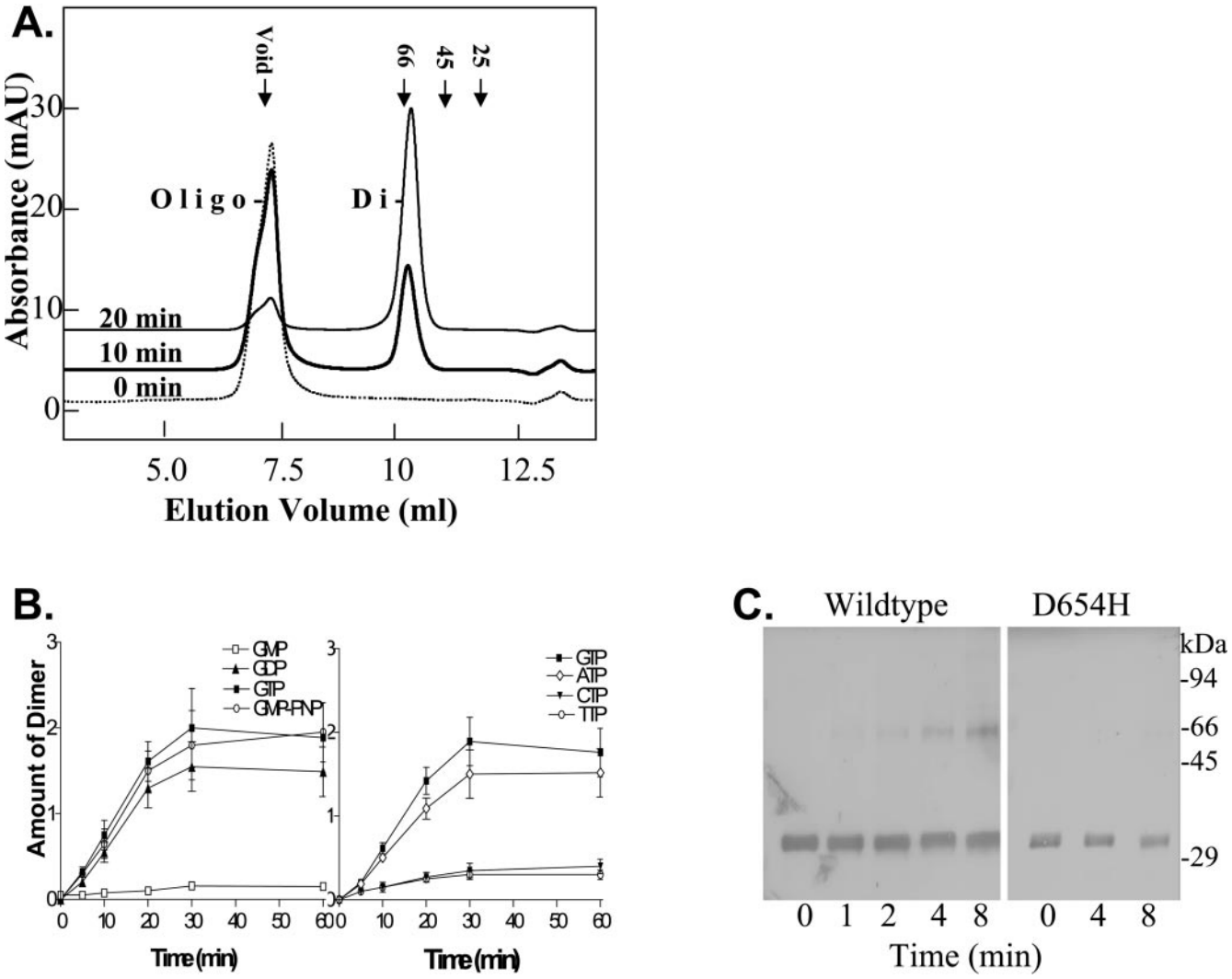

FIG. 2. Formation of CvaB CTD dimers from oligomers induced by nucleotides. (A) GTP-Mg (10 mM) was incubated with CvaB CTD oligomers in HEPES buffer on ice for various times; only data taken at 0 (dotted line), 10 (bold line), or 20 (thin line) min are shown (the oligomer and dimer were located at 7.12 and 10.02 ml, respectively). (B) Effects of different nucleotides on dimer formation (the amount of dimer is indicated as scanning data from Western blots; different sets of data were normalized.). (C) Lack of dimer formation by the nucleotide binding-defective D654H mutant protein.

oligomer fraction was about 1.68, implying that nearly no nucleotide was bound. The bound nucleotides in the dimer form were confirmed by thin-layer chromatography (TLC). Both the nucleotide diphosphates (minor) and nucleotide triphosphates (major) were found in the dimer but not in the oligomer (Fig. 1D). These results suggested that the bound nucleotide(s) was strongly associated with the dimer and might be critical for the formation of the CvaB CTD dimer.

Induction of dimers from oligomers by nucleotide binding. To identify the effect of nucleotide binding on protein dimerization, the purified nucleotide-free CvaB CTD oligomers were incubated with different nucleotides. The relative dimer and oligomer amounts were then detected by gel filtration chromatography. Based on our previous finding that the CvaB CTD bound GTP much better than ATP at low temperatures (49), we used GTP-Mg, attempting to convert the CvaB CTD from an oligomer to a dimer. As the time of GTP-Mg incubation on ice increased, the proportion of the oligomer decreased while that of the dimer increased (Fig. 2A). These results indicated that the nucleotide binding to the CvaB CTD induced the oligomers into dimers. This induction was rapid; about 80% of the dimer form appeared after 20 min.

To determine whether other nucleotides might induce the formation of CvaB CTD dimers, different nucleotides were tested. Almost no dimer was obtained with GMP. However, GDP, GTP, and GMP-PNP displayed similar induction rates for the CvaB CTD (Fig. 2B, left), indicating that the equilibrium of the monomer and dimer was not directly dependent on the hydrolysis of nucleotides from the triphosphate to the diphosphate. ATP and GTP displayed similar induction rates for the CvaB CTD. However, CTP and TTP showed a much lower rate than that of ATP or GTP (Fig. 2B, right). These results indicated that the purine base of the nucleotide is important for binding to ABC NBDs. This finding is consistent with our previous report that the radio-

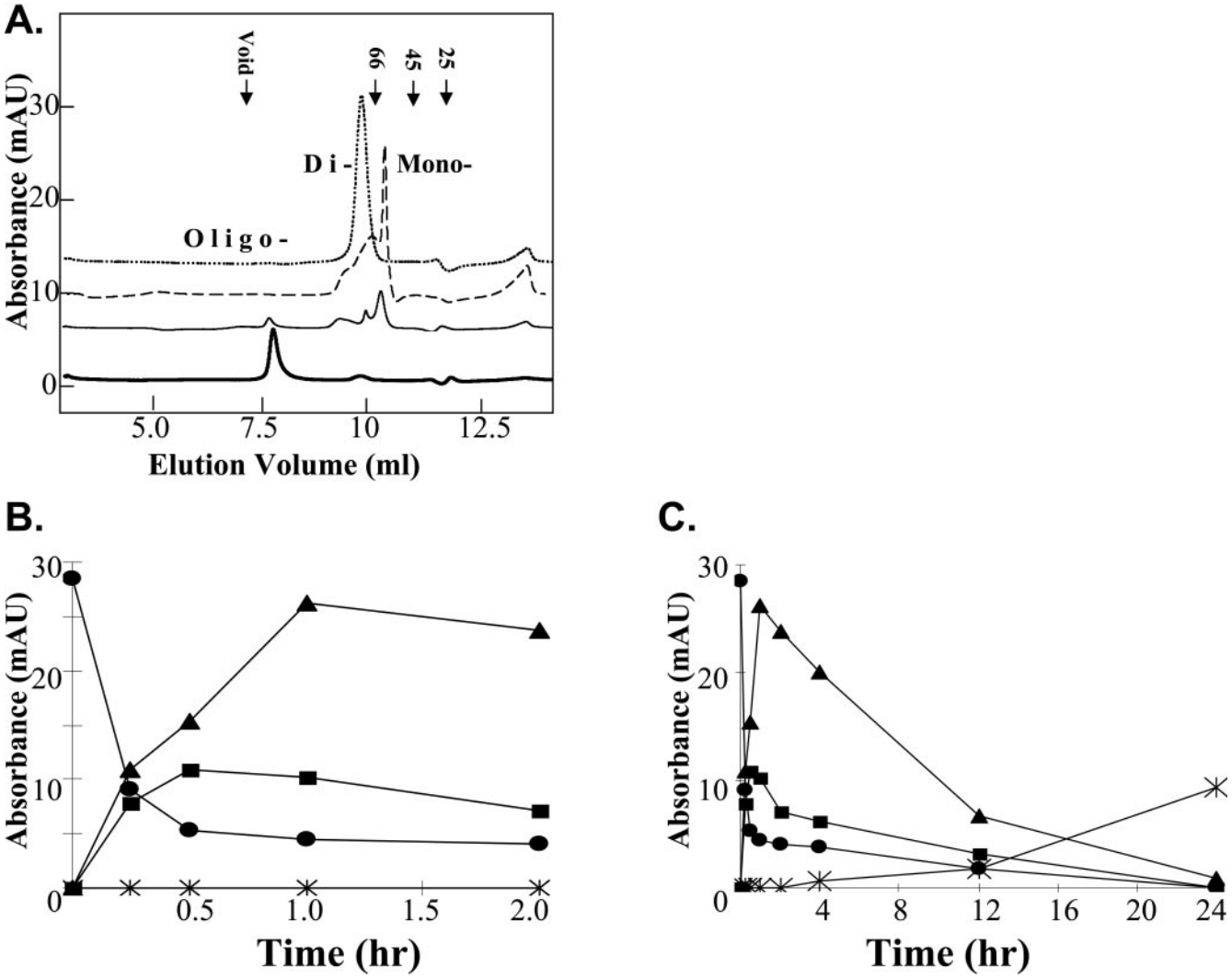

FIG. 3. Conversion of dimers to oligomers by chelation of Mg^{2+}. (A) Effects of removal of nucleotides. Different forms of the CvaB CTD shown with EDTA chelation for 0 (dotted line), 1 (dashed line), 4 (thin line), or 24 (bold line) h (the oligomers, dimers, and monomers were located at 7.2, 10.3, and 11.2 ml, respectively). (B) Rapid conversion of dimers to monomers upon removal of nucleotides. (C) Slow conversion to oligomers. The relative amounts of oligomer (star), dimer (circle), intermediate (square), and monomer (triangle) proteins are indicated by the peak heights.

active GTP-bound CvaB CTD could not be competed by 100 μM unlabeled CTP or UTP but was partially competed by ATP or ADP and highly competed by GTP or GDP (49).

To further demonstrate the importance of nucleotide binding for the function of the CvaB CTD, we determined the oligomer state by EDC cross-linking on the D654H defective mutant, which has a point mutation in the Walker B site of CvaB that severely impairs both nucleotide triphosphatase activities and nucleotide binding and completely abolished the secretion of colicin V (49). The wild-type CvaB CTD dimer could be cross-linked by EDC in a short time at room temperature (25°C), and more dimers were obtained with increased EDC cross-linking time (Fig. 2C, left). However, the nucleotide binding-defective D654H mutant did not form dimers; no dimer band was detected on EDC cross-linking (Fig. 2C, right). These results indicated that nucleotide binding was important for the CvaB CTD to be in the dimer form.

Monomers and oligomers induced by nucleotide removal from dimers. During these studies, it was found that oligomer forms appeared in the purified dimer fraction of the CvaB CTD upon storage at 4°C in HEPES buffer, and a low concentration of EDTA (5 mM) could greatly accelerate this oligomerization process. To further investigate the role of bound nucleotides on maintaining the dimer form of the CvaB CTD, EDTA was used to chelate the magnesium ion from the nucleotide-bound dimer, resulting in eventual nucleotide release from the CvaB CTD. To accelerate magnesium chelation, the temperature was set at 20°C and CAPS buffer (pH 10.4) was used, under which conditions the EDTA was fully deprotonated as the most efficient chelator (46). By analyzing the protein samples with increased time of EDTA chelation on gel filtration chromatography, it was found that the main fraction of the CvaB CTD shifted from dimers to monomers. Some intermediate forms were also observed in the first 2 h (Fig. 3A

and B). After 4 h of EDTA incubation, the oligomer appeared; by 24 h of EDTA incubation, only the oligomer form could be detected and almost half of the protein was lost, presumably due to protein aggregation (Fig. 3A). In comparison with the CvaB CTD dimerization induced by GTP-magnesium (Fig. 3A), this oligomerization due to nucleotide release was relatively slow (Fig. 3C). Nevertheless, it is clear that the oligomer and dimer forms of the CvaB CTD are interconvertible under different conditions and that nucleotide binding is critical for maintaining the dimer form.

Proximity of the Walker A site and the ABC signature motif shown by disulfide cross-linking. Shown in some ABC transporters, the highly specific ABC signature motif is adjacent to the nucleotide-binding pocket (Walker A and B sites) and functions to couple the nucleotide binding and conformational changes in TMDs (31, 39). To test the relative locations of the Walker A ($GASGA^{530}GKT$) site and the signature motif ($L^{630}SGGQ$) in CvaB CTD dimers, A530C and L630C site-direct mutagenesis, based on experimental data obtained with the human P glycoprotein (31), was done and disulfide cross-linking by oxidative copper phenanthroline was performed. As a control, the wild-type CvaB CTD was treated by oxidation under the same conditions. No disulfide-cross-linked dimer band was obtained under the oxidative condition (Fig. 4A, lane 1), even though each had four cysteine residues. Without nucleotide, A530C or L630C mutant protein or a mixture of the two at a ratio of 1:1 showed only monomer bands on SDS-PAGE (lanes 2 to 4). However, with nucleotide (GTP) preincubation, the mixture of L530C and L630C mutant proteins showed both monomer and dimer bands (lane 7); the dimer band disappeared when the sample was treated with 100 mM DTT after disulfide cross-linking (lane 8). The time course of the mixture of A530C and L630C mutant proteins in disulfide cross-linking is shown in Fig. 4B. These results indicate that the nucleotide binding induced a dimer form in which the Walker A site and the signature motif from two monomers were spatially proximal.

The observation that the A503C or L630C mutant protein individually did not show the disulfide-cross-linked dimer band (lanes 5 and 6 in Fig. 4A) but the mutant mixture did (lane 7) suggested that neither the two Walker A sites nor the two ABC signature motifs were spatially close to each other in the CvaB CTD dimer. These data indicated that the Walker A site and the signature motif were close enough to be cross-linked only when they were from different monomers.

Head-to-tail model of the nucleotide-dependent CvaB CTD dimer. To describe the effect of nucleotide binding on CvaB CTD dimerization, homology models of both the monomer and dimer forms of CTD were made (12, 13) with the crystal structures of the HlyB NBD as the template (36, 47). In addition, crystal structures of nucleotide-bound MJ0796 (45) and MalK (5, 7) were compared. A sandwich-like homodimer model of the CvaB CTD was obtained (Fig. 5A). By analyzing the models, it was found that the Walker A site and the signature motif were located far apart in a CvaB CTD monomer. The shortest separation was as long as 22.4 Å, indicating no direct interaction within a monomer. However, in the CvaB CTD dimer model, the monomers were in a head-to-tail arrangement, with two nucleotides sandwiched between Ala^{530} in the Walker A site of one monomer and Leu^{630} in the signature motif of the other (Fig. 5B). The Walker A site and ABC signature motif from different monomers formed two identical or very similar nucleotide-binding pockets in a CvaB CTD dimer. Shown in the dimer model, the selected residues (Ala^{530} and Leu^{630}) were within a 10-Å separation with side chains directed toward each other to facilitate disulfide bond formation once they were replaced by cysteines. As the functional form, the CvaB CTD homodimer was very possibly maintained by the interactions between subunits in nucleotide-binding pockets. We concluded that the nucleotide-dependent dimers were formed in a head-to-tail arrangement (Fig. 5A).

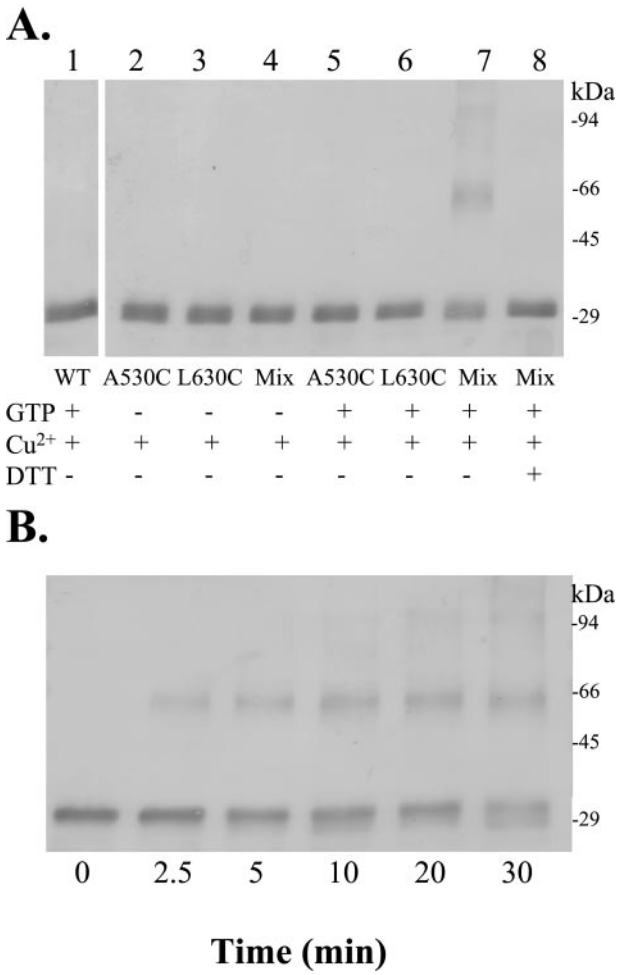

FIG. 4. The proximity of the Walker A site and ABC signature motif in the nucleotide-bound dimer. (A) Mixture of mutant proteins A530C and L630C can be disulfide cross-linked. Cu^{2+} is oxidative $[Cu(1,l0\text{-phenanthroline})_3]^{2+}$; 100 mM DTT was added to the mixture after disulfide cross-linking where indicated. (B) Time course of a mixture of A530C and L630C mutant proteins with 10 mM GTP oxidation at 37°C. WT, wild type.

DISCUSSION

In this study, the nucleotide-bound CvaB CTD was identified as a dimer, nucleotide binding was found to be critical for CTD dimerization, and nucleotide release from the dimer was found to result in the formation of monomers and oligomers.

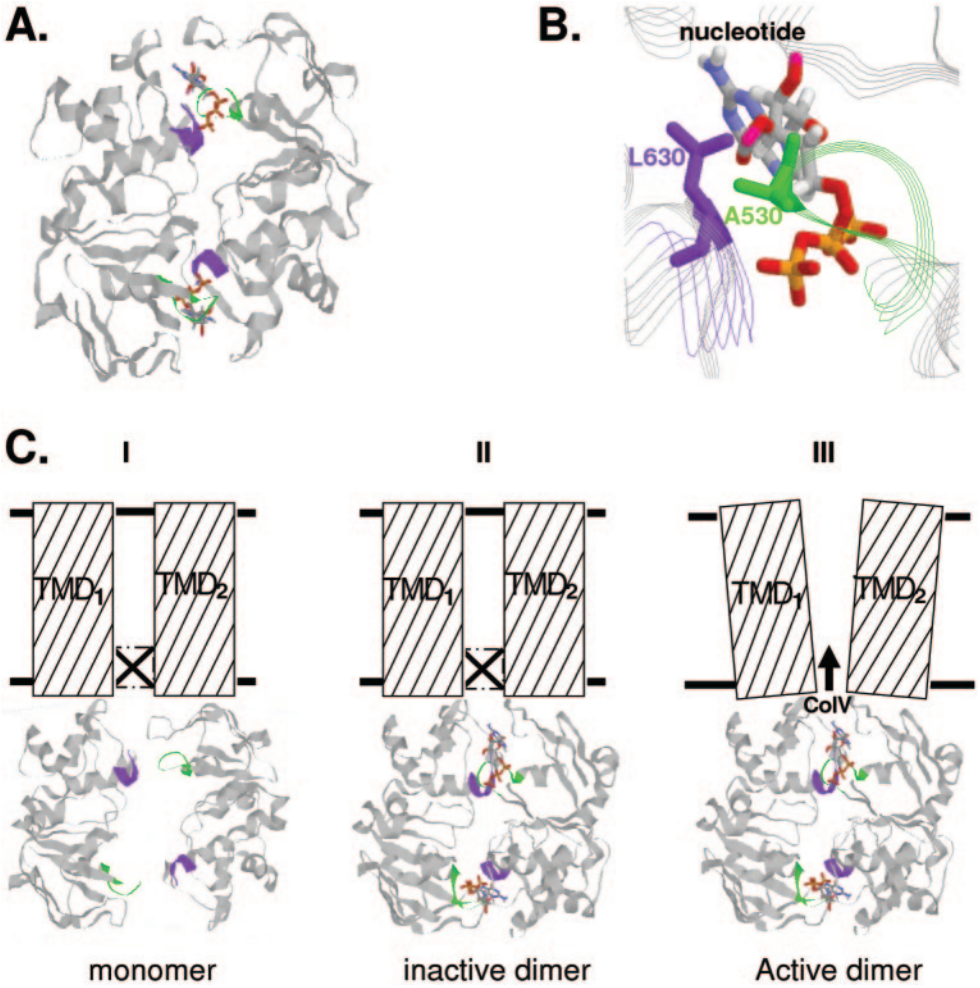

FIG. 5. Models of CvaB CTD dimers in colicin V secretion. (A) Model of the head-to-tail dimer (green, Walker A site; purple, signature motif). (B) Locations of A530 and L630 at the dimer interface with bound nucleotide. (C) Schematic representations of coupling of the nucleotide-dependent CTD dimerization to different states of ColV secretion exporter. I, monomeric transition state without nucleotide binding; II, nucleotide-bound inactive dimer in the absence of substrate ColV; III, active dimer in which ColV binding opens the CvaB channel. The closed and open states of the cytoplasmic channel are indicated by the cross and the arrow, respectively.

Site-directed mutagenesis and disulfide cross-linking studies verified that nucleotide binding drives the formation of a head-to-tail dimer in which the Walker A site and the ABC signature motif from different subunits are spatially close to each other.

The monomer and dimer forms are in equilibrium in the ABC NBDs of HlyB (1) and OpuAA (20). In this study, equilibrium of the monomer, dimer, and oligomer forms was observed in the CvaB CTD in vitro and nucleotide binding was found to have a critical role in this equilibrium. The oligomeric state of the CvaB CTD was converted into dimers rapidly with the purine nucleotide diphosphates and triphosphates (Fig. 2A and B), while the nucleotide binding-defective mutant protein was not (Fig. 2C). With the removal of nucleotides, the dimer form of the CvaB CTD was converted transiently and rapidly into monomers (Fig. 3A and B). Both nucleotide diphosphates and triphosphates were found in the purified CvaB CTD dimer, with triphosphates being the dominant form (Fig. 1D). Furthermore, the CvaB CTD dimers can be induced by both diphosphate and triphosphate purine nucleotides (Fig. 2B). Diphosphate nucleotides are widely used in crystallizing ABC NBDs (5, 9, 26). However, the nucleotide triphosphate has also been used to crystallize some ABC NBD dimers, such as MJ0796 (45), GlcV (43), Rad50 (19), and MalK (7). In this study, we found that CvaB CTD dimerization can be induced by both GTP and GDP, but not by GMP. Furthermore, different nucleotide triphosphates, such as ATP and GTP, can promote the formation of the CvaB CTD dimer at similar rates (Fig. 2B). The nucleotides with pyrimidine rings (CTP and UTP) had no effect on the oligomeric state of the CvaB CTD, which confirmed our previous result for the competitive binding of nucleotides (49). In vitro, the monomers oligomerized slowly and all were converted into oligomers and aggregates eventually (Fig. 3A and C). However, such oligomerization probably does not occur in vivo for several reasons. First, in whole CvaB, the CTD is merged with TMDs that integrate into the cytoplasmic membrane with the CTD in the cytoplasm. When the CvaB dimer is dissociated, the hydrophobic CvaB CTD monomers might partially interact with the membrane so

that oligomers cannot form. Second, in cells under physiological conditions, there is a high concentration of ADP or ATP and GDP or GTP in vivo, where nucleotides can promote the formation of the CvaB CTD dimer.

In most ABC transporters, nucleotide binding and hydrolysis by NBDs result in conformational changes in TMDs which open the cytoplasmic membrane channel for the secretion of substrates (3, 4, 32, 33). In addition to the ABC transporter CvaB, the ColV secretion system contains the outer membrane tunnel protein TolC and the accessory protein CvaA. To describe the role of nucleotide binding and hydrolysis in ColV secretion, three states of the CvaB CTD (monomer, inactive dimer, and active dimer) are proposed here (Fig. 5C). With no bound nucleotide, the CvaB CTD exists as monomers (Fig. 5C, part I); once a nucleotide is bound, the CvaB CTD will be in a dimer form. Considering that a high concentration of nucleotides exists in vivo and different nucleotides (GTP, GDP, ATP, and ADP) can induce CvaB CTD dimerization, the CTD monomers may be just a transient state. The nucleotide triphosphate was found to dominate in the CTD dimer, suggesting low-level nucleotide triphosphate hydrolysis in vitro. However, ColV precursor processing requires energy from nucleotide binding and hydrolysis. Thus, we propose that there are two states of CvaB dimer, i.e., inactive and active forms. In an inactive CvaB dimer (Fig. 5C, part II), even bound with nucleotides, the cytoplasmic CvaB channel is closed. Only when the substrate (ColV) binds to the CvaB TMD and in the presence of CvaA and TolC, the ATP- or GTP-bound CvaB dimer becomes active (Fig. 5C, part III) and the channel is open for export of the substrate ColV.

Nucleotide hydrolysis provides energy for substrate secretion. Two proposals have been described for the roles of nucleotide hydrolysis in ABC-involved exporters. First, nucleotide hydrolysis directly promotes ABC channel opening for secretion. Secondly, nucleotide hydrolysis occurs after substrate secretion for initiation of the next cycle. In the first proposal, as previously described (8, 16, 24), the CvaB dimer is in an inactive state without substrate binding (Fig. 5C, part II). Binding of the substrate ColV stimulates nucleotide triphosphate binding and consequent hydrolysis to a CvaB dimer (Fig. 5C, part III), which provides energy for conformational changes in CvaB TMDs and for opening of the ABC channel for substrate export. However, several recent studies indicated that it is the binding, rather than the hydrolysis, of nucleotide triphosphate that provides the power stroke for ABC-involved export (32, 44). Thus, in the second proposal, the binding of nucleotide diphosphates and triphosphates marks the lower-energy and high-energy states of the CvaB dimer, respectively. When the nucleotide diphosphate is bound, the CTD dimer is in an inactive state and the CvaB cytoplasmic channel is closed (Fig. 5C, part II). Substrate (ColV) binding promotes the replacement of nucleotide diphosphates with nucleotide triphosphates on CTDs. Nucleotide triphosphate binding to CTDs results in a high-energy active form of CvaB dimer (Fig. 5C, part III) for substrate export. After secretion, the bound nucleotide triphosphate is hydrolyzed, the CvaB active dimer changes back into an inactive low-energy status, and the ABC channel becomes closed. Regardless of when nucleotide hydrolysis takes place, only the active form of the channel composed of CvaA, CvaB, and TolC allows secretion of the bound substrate ColV.

ACKNOWLEDGMENTS

This work was supported in part by National Institutes of Health research grants GM34766 (P.C.T.) and GM65762 (R.W.H.), the Georgia Cancer Coalition (R.W.H.), a Molecular Basis of Disease Program fellowship (X.G.), and Research Enhancement Program funds from Georgia State University. The facilities were supported by funds obtained through the Georgia Research Alliance.

REFERENCES

1. **Benabdelhak, H., L. Schmitt, C. Horn, K. Jumel, M. A. Blight, and I. B. Holland.** 2005. Positive co-operative activity and dimerization of the isolated ABC ATPase domain of HlyB from Escherichia coli. Biochem. J. **386:**489–495.
2. **Bobadilla, J. L., M. Macek, J. P. Fine, and P. M. Farrell.** 2002. Cystic fibrosis: a worldwide analysis of CFTR mutations—correlation with incidence data and application to screening. Hum. Mutat. **19:**575–606.
3. **Chang, G.** 2003. Structure of Msba from Vibrio cholerae: a multidrug resistance ABC transporter homolog in a closed conformation. J. Mol. Biol. **330:**419–430.
4. **Chang, G., and C. B. Roth.** 2001. Structure of Msba from E. coli: a homolog of the multidrug resistance ATP binding cassette (ABC) transporters. Science **293:**1793–1800.
5. **Chen, J., G. Lu, J. Lin, A. L. Davidson, and F. A. Quiocho.** 2003. A tweezers-like motion of the ATP-binding cassette dimer in an ABC transport cycle. Mol. Cell **12:**651–661.
6. **Dean, M.** 2002. The human ATP-binding cassette (ABC) transporter superfamily. National Center for Biotechnology Information website. http://www.ncbi.nlm.nih.gov/books/bv.fcgi?call=bv.View..ShowTOC&rid=mono_001.TOC&depth=2.
7. **Diederichs, K., J. Diez, G. Greller, C. Mueller, J. Breed, C. Schnell, C. Vonrhein, W. Boos, and W. Welte.** 2000. Crystal structure of MalK, the ATPase subunit of the trehalose/maltose ABC transporter of the archaeon Thermococcus litoralis. EMBO J. **19:**5951–5961.
8. **Dong, J., G. Yang, and H. S. Mchaourab.** 2005. Structural basis of energy transduction in the transport cycle of MsbA. Science **308:**1023–1028.
9. **Gaudet, R., and D. C. Wiley.** 2001. Structure of the C-terminal ABC ATPase domain of human Tap1, the transporter associated with antigen processing. EMBO J. **20:**4964–4972.
10. **Gilson, L., H. K. Mahanty, and R. Kolter.** 1990. Genetic analysis of an MDR-like export system: the secretion of colicin V. EMBO J. **9:**3875–3894.
11. **Hanahan, D.** 1983. Studies on transformation of Escherichia coli with plasmids. J. Mol. Biol. **166:**557–580.
12. **Harrison, R. W.** 1999. A self-assembling neural network for modeling polymer structure. J. Math. Chem. **26:**125–137.
13. **Harrison, R. W., D. Chatterjee, and I. T. Weber.** 1995. Analysis of six protein structures predicted by comparative modeling techniques. Proteins **23:**463–471.
14. **Higgins, C. F., I. D. Hiles, G. P. Salmond, D. R. Gill, J. A. Downie, I. J. Evans, I. B. Holland, L. Gray, S. D. Buckel, A. W. Bell, M. A., and M. A. Hermodson.** 1986. A family of related ATP-binding subunits coupled to many distinct biological processes in bacteria. Nature **323:**448–450.
15. **Higgins, C. F., and K. J. Linton.** 2004. The ATP switch model for ABC transporters. Nat. Struct. Mol. Biol. **11:**918–926.
16. **Holland, I. B., and M. A. Blight.** 1999. ABC-ATPases, adaptable energy generators fuelling transmembrane movement of a variety of molecules organisms from bacteria to humans. J. Mol. Biol. **293:**381–399.
17. **Holland, I. B., and M. A. Blight.** 1996. Structure and function of HlyB, the ABC-transporter essential for haemolysin secretion from Escherichia coli, p. 111–135. *In* W. N. Konings, H. R. Kaback, and J. S. Lolkema (ed.),The handbook of biological physics. Volume 2. Transport processes in eukaryotic and prokaryotic organisms . Elsevier Press, New York, N.Y.
18. **Holland, I. B., S. P. C. Cole, K. Kuchler, and C. F. Higgins.** 2003. ABC proteins: from bacteria to man. Academic, London, United Kingdom.
19. **Hopfner, K. P., A. Karcher, D. S. Shin, L. Craig, L. M. Arthur, J. P. Carney, and J. A. Tainer.** 2000. Structural biology of Rad50 ATPase: ATP-driven conformational control in DNA double-strand break repair and the ABC-ATPase superfamily. Cell **101:**789–800.
20. **Horn, C., E. Bremer, and L. Schmitt.** 2003. Nucleotide dependent monomer/dimer equilibrium of OpuAA, the nucleotide-binding protein of the osmotically regulated ABC transporter OpuA from Bacillus subtilis. J. Mol. Biol. **334:**403–419.
21. **Horton, R. M.** 1993. *In vitro* recombination and mutagenesis of DNA: SOEing together tailor-made genes, p. 251–262. *In* B. A. White (ed.), Methods in molecular biology, vol. 15. Humana Press, Totowa, N.J.
22. **Hung, L. W., I. X. Wang, K. Nikaido, P. Q. Liu, G. F. L. Ames, and S. H. Kim.** 1998. Crystal structure of the ATP-binding subunit of an ABC transporter. Nature **396:**703–707.

23. **Hwang, J. W., X. T. Zhong, and P. C. Tai.** 1997. Interactions of dedicated export membrane proteins of the colicin V secretion system: CvaA, a member of the membrane fusion protein family, interacts with CvaB and TolC. J. Bacteriol. **179:**6264–6270.
24. **Janas, E., M. Hofacker, M. Chen, S. Gompf, C. van der Does, and R. Tampe.** 2003. The ATP hydrolysis cycle of the nucleotide-binding domain of the mitochondrial ATP-binding cassette transporter Mdl1p. J. Biol. Chem. **278:** 26862–26869.
25. **Jones, P. M., and A. M. George.** 2004. The ABC transporter structure and mechanism: perspectives on recent research. Cell. Mol. Life Sci. **61:**682–699.
26. **Karpowich, N., O. Martsinkevich, L. Linda Millen, Y.-R. Yuan, P. L. Dai, K. MacVey, P. J. Thomas, and J. F. Hunt.** 2001. Crystal structures of the MJ1267 ATP-binding cassette reveal an induced-fit effect at the ATPase active site of an ABC transporter. Structure **9:**571–586.
27. **Laemmli, U. K.** 1970. Cleavage of structural proteins during the assembly of the head of bacteriophage T4. Nature **227:**680–685.
28. **Lewis, H. A., S. G. Buchanan, S. K. Burley, K. Conners, M. Dickey, M. Dorwart, R. Fowler, X. Gao, W. B. Guggino, W. A. Hendrickson, J. F. Hunt, M. C. Kearins, D. Lorimer, P. C. Maloney, K. W. Post, K. R. Rajashankar, M. E. Rutter, J. M. Sauder, S. Shriver, P. H. Thibodeau, P. J. Thomas, M. Zhang, X. Zhao, and S. Em.** 2004. Structure of nucleotide-binding domain 1 of the cystic fibrosis transmembrane conductance regulator. EMBO J. **23:** 282–293.
29. **Locher, K. P.** 2004. Structure and mechanism of ABC transporters. Curr. Opin. Struct. Biol. **14:**426–431.
30. **Locher, K. P., A. T. Lee, and D. C. Rees.** 2002. The E. Coli Btucd structure: a framework for ABC transporter architecture and mechanism. Science **296:**1091–1098.
31. **Loo, T. W., M. C. Bartlett, and D. M. Clarke.** 2002. The "LSGGQ" motif in each nucleotide-binding domain of human P-glycoprotein is adjacent to the opposing Walker A sequence. J. Biol. Chem. **277:**41303–41306.
32. **Oloo, E. O., and D. P. Tieleman.** 2004. Conformational transitions induced by the binding of MgATP to the vitamin B_{12} ATP-binding cassette (ABC) transporter BtuCD. J. Biol. Chem. **279:**45013–45019.
33. **Reyes, C. L., and G. Chang.** 2005. Structure of the ABC transporter MsbAin complex with ADP. Vanadate and lipopolysaccharide. Science **308:**1028–1031.
34. **Samanta, S., T. Ayvaz, M. Reyes, H. A. Shuman, J. Chen, and A. L. Davidson.** 2003. Disulfide cross-linking reveals a site of stable interaction between C-terminal regulatory domains of the two MalK subunits in the maltose transport complex. J. Biol. Chem. **278:**35265–35271.
35. **Sambrook, J., E. F. Fritsch, and T. Maniatis.** 1989. Molecular cloning: a laboratory manual, 2nd ed. Cold Spring Harbor Laboratory Press, Cold Spring Harbor, N.Y.
36. **Schmitt, L., H. Benabdelhak, M. A. Blight, I. B. Holland, and M. T. Syubbs.** 2003. Crystal Structure of the nucleotide binding domain of the ABC-transporter haemolysin B: identification of a variable region within ABC helical domains. J. Mol. Biol. **330:**333–342.
37. **Schmitt, L., and R. Tampé.** 2002. Structure and mechanism of ABC transporters. Curr. Opin. Struct. Biol. **12:**754–760.
38. **Schneider, E., and S. Hunke.** 1998. ATP-binding-cassette (ABC) transport systems: functional and structural aspects of the ATP-hydrolyzing subunits/domains. FEMS Microbiol. Rev. **22:**1–20.
39. **Shyamala, V., V. Baichwal, E. Beall, and G. F. Ames.** 1991. Structure-function analysis of the histidine permease and comparison with cystic fibrosis mutations. J. Biol. Chem. **266:**18714–18719.
40. **Studier, F. W., and B. A. Moffatt.** 1986. Use of bacteriophage T7 RNA polymerase to direct selective high-level expression of cloned genes. J. Mol. Biol. **189:**113–130.
41. **van Belkum, M. J., R. W. Worobo, and M. E. Stiles.** 1997. Double-glycine-type leader peptides direct secretion of bacteriocins by ABC transporters: colicin V secretion in Lactococcus lactis. Mol. Microbiol. **23:**1293–1301.
42. **Verdon, G., S. V. Albers, B. W. Dijkstra, A. J. Driessen, and A. M. Thunnissen.** 2003. Crystal structures of the ATPase subunit of the glucose ABC transporter from Sulfolobus solfataricus: nucleotide-free and nucleotide-bound conformations. J. Mol. Biol. **330:**343–358.
43. **Verdon, G., S. V. Albers, N. van Oosterwijk, B. W. Dijkstra, A. J. Driessen, and A. M. Thunnissen.** 2003. Formation of the productive ATP-Mg^{2+}-bound dimer of GlcV, an ABC-ATPase from Sulfolobus solfataricus. J. Mol. Biol. **334:**255–267.
44. **Vergani, P., S. W. Lockless, A. C. Nairn, and D. C. Gadsby.** 2005. CFTR channel opening by ATP-driven tight dimerization of its nucleotide-binding domains. Nature **433:**876–880.
45. **Yuan, Y., S. Blecker, O. Martsinkevich, L. Millen, P. J. Thomas, and J. F. Hunt.** 2001. The crystal structure of the MJ0796 ATP-binding cassette: implications for the structural consequences of ATP hydrolysis in the active site of an ABC-transporter. J. Biol. Chem. **276:**32313–32321.
46. **Zaitseva, J., I. B. Holland, and L. Schmitt.** 2004. The role of CAPS buffer in expanding the crystallization space of the nucleotide-binding domain of the ABC transporter haemolysin B from Escherichia coli. Acta Crystallogr. D Biol. Crystallogr. **60:**1076–1084.
47. **Zaitseva, J., S. Jenewein, T. Jumpertz, B. Holland, and L. Schmitt.** 2005. H662 is the linchpin of ATP hydrolysis in the nucleotide-binding domain of the ABC transporter HlyB. EMBO J. **24:**1901–1910.
48. **Zaitseva, J., S. Jenewein, A. Wiedenmann, H. Benabdelhak, I. B. Holland, and L. Schmitt.** 2005. Functional characterization and ATP-induced dimerization of the isolated ABC-domain of the haemolysin B transporter. Biochemistry **44:**9680–9690.
49. **Zhong, X., and P. C. Tai.** 1998. When an ATPase is not an ATPase: at low temperatures the CTD of the ABC transporter CvaB is a GTPase. J. Bacteriol. **180:**1347–1353.